DROP-IT

DELIVERABLE 1.4

Polycrystalline thin films of B-LFP from molecular precursors and properties

Due date of deliverable: 2020/10/31

Actual submission date: 2020/12/21

Deliverable number:	D1.4
Due date:	30.10.2019
Nature[1]:	R
Dissemination Level[1]:	PU
Work Package:	WP1
Lead Beneficiary:	UJI
Contributing Beneficiaries:	SRI, UVEG

---

[1] **Nature:** R = Report, P = Prototype, D = Demonstrator, O = Other
Dissemination level PU = Public PP = Restricted to other programme participants (including the Commission Services) RE = Restricted to a group specified by the consortium (including the Commission Services) CO = Confidential, only for members of the consortium (including the Commission Services) Restraint UE = Classified with the classification level "Restraint UE" according to Commission Deci-sion 2001/844 and amendments Confidential UE = Classified with the mention of the classification level "Confidential UE" according to Commission Decision 2001/844 and amendments Secret UE = Classified with the mention of the classification level "Secret UE" according to Commis-sion Decision 2001/844 and amendments

This project has received funding from the European Union's Horizon 2020 research and innovation programme under **Grant Agreement No. 862656**.

DOCUMENT HISTORY

Version	***Date***	***Reason of change***
1	2020/12/02	SRI
2	2020/12/04	UJI – complete version
3	2020/12/08	Revised version by SRI and UJI
4	2020/12/21	Last edition/revision by UVEG

Table of Content

This project has received funding from the European Union's Horizon 2020 research and innovation programme under **Grant Agreement No. 862656**.

1 Aim of the deliverable

The aim of the deliverable D1.4 entitled “In-situ synthesis of LFP thin films from molecular precursors” is the deposition of thin films deposited by spin coating, to speed up the determination of parameters related to B-/G-LFP formation/growth. Soft Chemistry routes are used to prepare homogeneous thin films of polycrystalline G-LFPs proposed, starting from the most common $FASnI_3$ LFP material. This task is propaedeutic for the optimization process for inkjet (WP2) and device fabrication (WP3-WP5). Involved partners: UJI (leader, Synthesis of precursors, polycrystalline films, characterization), UVEG (exciton recombination dynamics, optical gain and photoconductivity). SRI (preparation of B-/G-LFP films, basic and specific characterization), INSA (beyond DFT refinement).

2 Introduction: description of work & main achievements

The Task 1.4 consisted in identifying benchmark composition of tin based perovskite leading to state-of-the-art efficiency and achieving pinhole free films, with state-of-the-art optoelectronic properties from molecular precursor. Several compositions based on $FASnI_3$ have been identified. The work was carried out in parallel by SRI and UJI. Briefly, the SRI work is based on GeI_2 doping and PEAI (phenethylammonium iodide) incorporation. SRI has deposited thin films on glass substrate by spin coating in a N_2 glovebox and characterized the layers using SEM, XRD and PL to extract information on the morphology of the samples, crystallinity and optoelectronic properties. The influence of different additives and solution concentration on thin film properties has been assessed. The main achievement realized by SRI is the deposition of pinhole free layers of benchmark Sn based perovskites with adapted bandgap for photovoltaic applications. The UJI work developed an exhaustive synthetic work focused on obtaining LFP ($FASnX_3$, X = I, Br) films by spin-coating. This was a preliminary step to the selection of the charge transport materials and the assembly of complete photovoltaic device and LEDs (WP3 - Task 3.2 and WP4 – Task 4.2/4.3, respectively). Moreover, these films were used in the WP5 to carry out preliminary experiments on optical waveguide amplifiers.

3 Results

3.1 Polycrystalline thin films of $FASnX_3$ from molecular precursors and properties

One of the challenges of Sn-Perovskites (Sn-Ps) is to hinder the oxidation of Sn^{2+} into its more stable state of Sn^{4+}, which produces Sn vacancies in the perovskite that are responsible for high levels of self p-doping. For this reason, Sn-Ps are very unstable at the contact with air and water. In the literature it is found the use of many additives to reduce this oxidation, such as, SnF_2, H_3PO_2, $SnCl_2$ or the mix of cations engineering. One of the most effective ways is the inclusion of 2D bulky cations, which increase the moisture stability, as previously demonstrated in solar cells based on 2D/3D perovskites [1]. For this reason, we introduced here the bulky cation Dipropil-ammonium iodide (DipI) to the LFP. Also, we included well known highly reducing agent, the sodium borohydride ($NaBH_4$) to the LFP's precursor solution (FAI and SnI_2). In Figure 1 top view SEM images show the morphology of LFP films with and without additives. The pure $FASnI_3$ film (Figure 1a) exhibits a poor morphology with some pinholes and small aggregates. It is worth noting that the reference sample is stable to carry out the characterization due to the presence of the SnF_2, together with the precursors (FAI and SnI_2). The film with $NaBH_4$ as additive (Figure 1b) also shows a very poor morphology with even more pinholes than the standard film, but the crystallinity is improved (Figure 1e). The effect of the DipI (Figure 1c) is beneficial as the morphology is more uniform and the grains are bigger and with a better crystallinity (Figure 1e), even if small pinholes are present. The addition of the two additives (DIpI and $NaBH_4$) to the $FASnI_3$, results in a film without pinholes (the black spots are due to residual $NaBH_4$) in the film, even though the grain size and the crystal quality decreases (Figure 1e). We fabricated devices with an inverted structure (ITO/PEDOT/perovskite/PCBM/BCP(Al)), with and without additives and we found that the best performance (5%) and stability (PCE stable for 180 min, without encapsulation, measured in ambient conditions) were achieved with the combination of the DipI and $NaBH_4$, demonstrating the good coverage of the thin perovskite film.

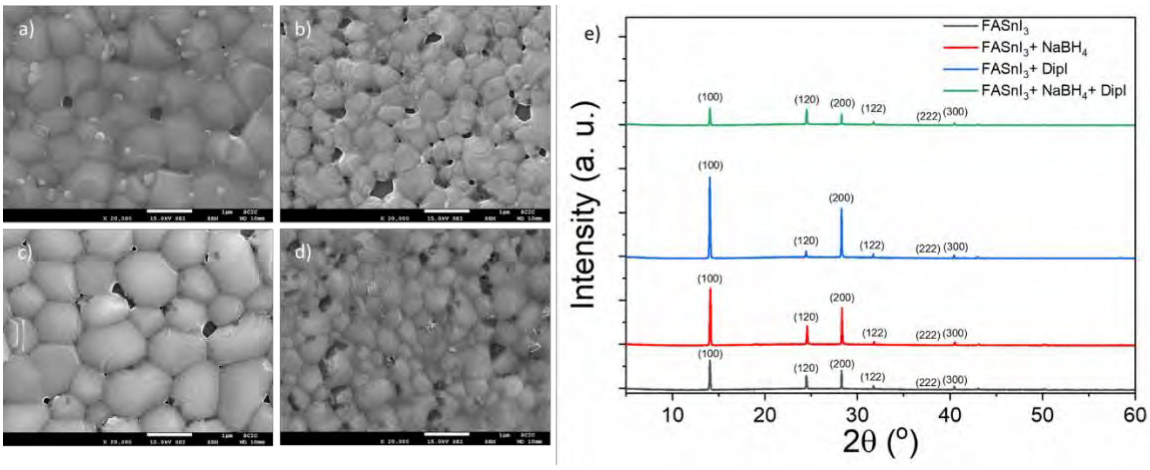

Figure 1. Morphological and crystallographic characterization of $FASnI_3$ thin films with different additives: SEM top view images of tin-perovskite of a) $FASnI_3$, b) $FASnI_3$ + $NaBH_4$, c) $FASnI_3$ + DipI, and d) $FASnI_3$ + $NaBH_4$ + DipI films, respectively; e) corresponding X-Ray diffraction patterns; the indexed diffraction peaks correspond to the orthorhombic lattice (Amm2 space group).

Moreover, this result highlights the importance of adding bulky cation. Thus, firstly we further passivate the perovskite surface with the fluor-phenethylammonium iodide (F-PEAI). The highest photoluminescence quantum yield (PLQY) is reached for the film with the combination of additives (Figure 2). The PL of the films with DipI show the features of a 2D/3D perovskite, as peaks at low wavelength appear.

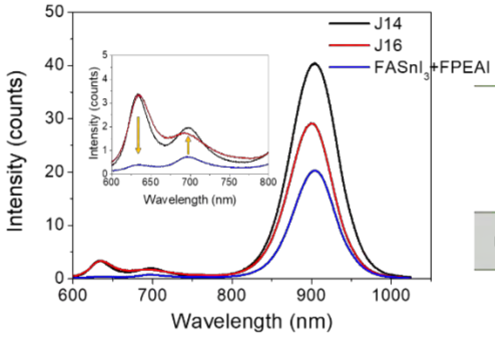

Samples	FASnI3 + NaBH4 + Dipral (n=10) + F-PEAI (J14)	FASnI3 + NaBH4 + Dipral (n=10) + Ácido ascórbico + F-PEAI (J16)	FASnI$_3$+FPEAI
PLQY (%)	1.35	0.96	0.60

Figure 2. Comparison between photoluinescence (PL) spectra@405nm registered with the CCD of the samples passivated with the F-PEAI.

Secondly, we used phenetylammonium iodide (PEAI) instead of the DIpI. **Figure 3** shows a series of Sn-based perovskites (PS) prepared with I and Br, respectively, and with different amounts of PEAI, determined by the parameter "n".

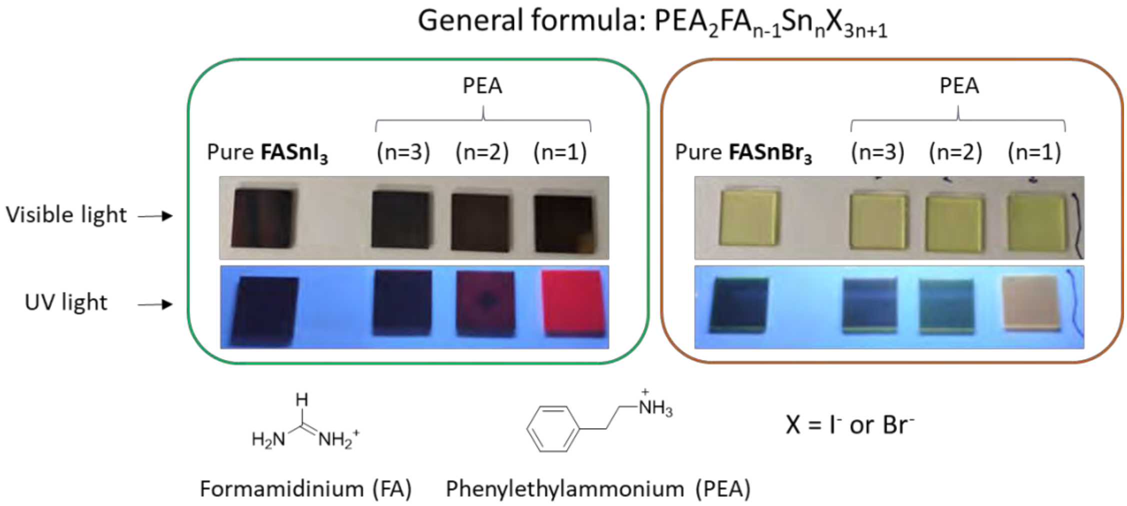

Figure 3. LFP perovskite films under visible and UV light prepared with different halides (I or Br) and different ratios of the organic cations (FA and PEA).

Clearly, the color of the films illuminated with visible light is determined by the composition and interestingly, the characteristic luminescence of some of these films can be observed upon illumination with UV light. To study the photoluminescent properties of these LFPs, the emission spectra and PLQY have been registered using an integrating sphere setup. It is worth mentioning that these experiments are being carried out currently and only those results from the iodide-based PS are presented. Figure 4 shows the luminescence spectra of the pure $FASnI_3$ and those derivatives with different amounts of PEAI following the formula $PEA_2FA_{n-1}Sn_nI_{3n+1}$.

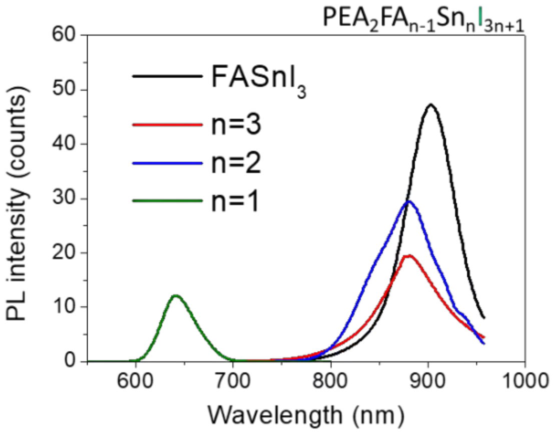

Figure 4. Luminescence spectra of $PEA_2FA_{n-1}Sn_nI_{3n+1}$ films with different FA/PEA ratios.

Table 1. PLQY of the LFP films based on iodide with different amounts of FA and PEA.

	PLQY (%)			
	Pure $FASnX_3$	**n = 3**	**n = 2**	**n = 1**
$PEA_2FA_{n-1}Sn_nI_{3n+1}$	1.39	0.72	1.02	0.22

As a general trend, the results displayed on Figure 4 and Table 1 indicate that the insertion of increasing amounts of the bulky cation PEA induces a notable shift of the emission maxima to visible wavelengths, accompanied with relatively significant decrease of the PLQY values. In order to better understand this behavior, the characterization of the bromide derivatives is being currently conducted and analyzed. Additionally, a deeper exploration of a series of these families of materials with broader compositions will be carried out in the future with the aim of providing a fully control over the spectral position of the luminescence and enhancement of the PLQY.

Upon characterization and selection of the most promising materials, the fabrication of complete solar cells and LEDs will be carried out for an optimization of the charge selective contacts, *i.e.* hole and electron transport materials (HTM and ETM), respectively, for a successful optimization of the device's efficiencies and performances.

3.2 Influence of additive in the preparation of polycrystalline thin films of $FASnI_3$ from molecular precursors

First, the influence of the additives used in Ref. 2 (reporting the efficiency world record of 13 % in solar cells based on $FASnI_3$) has been assessed. We have characterized in samples 1-4 of Table 2 the effect of introduction of GeI_2 (germanium diiodide), EAI (ethylammonium iodide) and $EDAI_2$ (ethylenediammonium diiodide) in $FASnI_3$. From the results presented in Table 2 it can be seen that combining GeI_2, EAI and $EDAI_2$ reduce the PL FWHM (photoluminescence spectra full width at half maximum), increase the PL average lifetime (photoluminescence carrier lifetime) and decrease the XRD FWHM (full width at half maximum of the (001) perovskite peak). These results show that these additives effectively reduce the defect density in $FASnI_3$ and increase the films crystallinity. Nevertheless, from the SEM layers presented on Figure 5 all the layers present large pinholes making these layers incompatible with making shunt-free device.

Table 2. Summary of the main processing condition layer parameter extract from the performed characterization. XRD FWHM, PL peak, PL FWHM and PL average lifetime refer to the full width at half maximum (FWHM) of the (001) perovskite peak, the position of the PL spectra peak, the FWHM of the PL spectra and carrier lifetime respectively.

Sample number	additive	Solution concentration	SnF_2 excess	XRD FWHM	PL peak	PL FWHM	PL average lifetime
				degree	eV	meV	ns
1	No	1M	10%	0.13	1.39	112	0.75
2	GeI_2	1M	10%	0.15	1.39	98	1.52
3	GeI_2, EAI	1M	10%	0.12	1.40	95	1.22
4	GeI_2, EAI,$EDAI_2$	1M	10%	0.11	1.40	96	1.41
5	No	0.8M	7.5%	0.12	1.39	159	0.40
6	PEAI	0.8M	7.5%	0.10	1.39	103	1.00
7	NH_4SCN	0.8M	7.5%	0.12	1.40	181	0.42
8	PEAI,NH_4SCN	0.8M	7.5%	0.10	1.38	98	1.41
9	PEAI,NH_4SCN	1M	7.5%	0.11	1.38	111	4.3
10	PEAI,NH_4SCN	1M	10%	0.10	1.38	110	4.5

Second, the influence of the additives used in Ref. 3 (reporting an efficiency of 12 % in solar cells based on $FASnI_3$) has been assessed. We have characterized in samples 5-10 from Table 2 the introduction of NH_4SCN (ammonium thiocyanate) and PEAI (phenethylammonium iodide). From the results presented in Table 1, combining NH_4SCN and PEAI decrease the PL FWHM, increase the PL average lifetime and decrease the XRD FWHM. These results show that these additives effectively reduce the defect density in $FASnI_3$ and increase the films crystallinity. Also, from the SEM layers presented in Figure 1 when PEAI is added it modified the layer morphology leading to smooth pinhole free films compatible with device manufacturing.

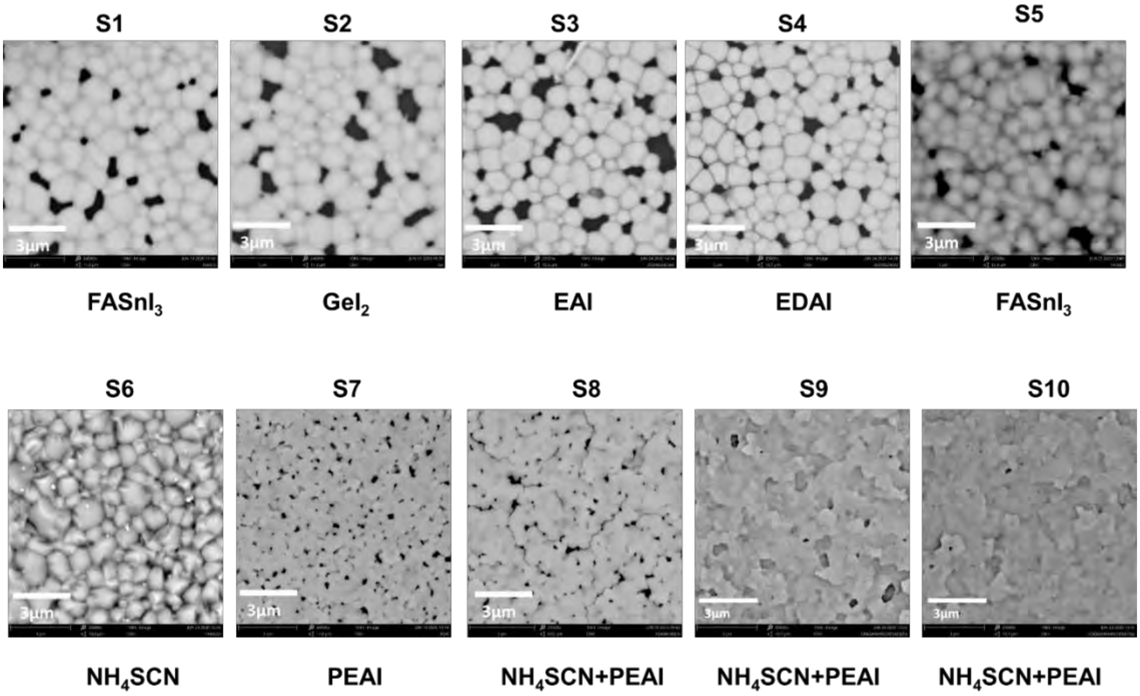

Figure 5. SEM images of Sn based BLFP thin film samples S1 to S10 (corresponding to the samples in Table 2).

Finally, we assessed the SnF_2 and solution concentration influence as the identified recipe were different on these two aspects. The recipe from [1] is using 10% excess of SnF_2 and 1M concentration while the recipe from [2] is using 7.5% excess of SnF_2 and 0.8M concentration. The results presented in table 1 seems to indicate that on the one hand the SnF_2 excess (sample 9 and 10) does not have a major impact on the film`s structural and optoelectronic properties as no significant change on the XRD and PL FWHM is observed. On the other hand, from the results presented in Table 2, it is evident that increasing the solution concentration leads to the PL FWHM increase, as well as the PL average lifetime increase accompanied by the XRD FWHM increase. These results show that decreasing the solution concentration from 1 to 0.8M effectively reduce the defect density in $FASnI_3$ and increase the films crystallinity. However, from the SEM images presented on Figure 5 increasing the precursor solution concentration to 1M seems to reduce the presence of pinholes, which might improve device performance increasing the shunt resistance.

Table 3 summarizes the influence of additive, precursor concentration and SnF_2 concentration influence on surface coverage, XRD intensity, XRD FWHM, PL lifetime and PL FWHM.

Table 3. Summary of additive, precursor concentration and SnF_2 concentration influence on surface coverage, XRD intensity, XRD FWHM, PL lifetime and PL FWHM.

+++ (very high), ++(high), + (slight improvement), - (no improvement)

Parameters		SEM Coverage	XRD intensity	XRD FWHM	PL Lifetime	PL FWHM
Additive	EAI	-	+	+	-	+
	EDAI	-	-	++	-	-
	GeI_2	-	-	-	++	++
	NH_4SCN	+++	-	-	+	-
	PEAI	++	+++	++	++	++
Solution concentration	0.8 M	-	-	-	-	+
	1 M	++	-	-	++	-
SnF_2 concentration	0.075 M	-	-	-	-	-
	0.1 M	+	-	-	-	-

4 Conclusions & Future directions

We have demonstrated the possibility to spin-coat (in glove box) and characterize $FASnX_3$ films from molecular precursors, as shown by the morphological, structural and optical properties. Considering the effects of several additives we recognized as the more stable and with best structural and optical properties the $FASnI_3$ film with DipI + $NaBH_4$ additives. With this film, solar cells were fabricated (in glove box) and a stable PCE of 5% was demonstrated (WP3). All characterization work was done under ambient conditions. The results are encouraging and we are moving to other perovskite element combinations to reach also good performances with LEDs.

5 References

[1] J. Rodríguez-Romero, J. Sanchez-Diaz, C. Echeverría-Arrondo, S. Masi, D. Esparza, E. M. Barea, and I. Mora-Seró, Widening the 2D/3D Perovskite Family for Efficient and Thermal-Resistant Solar Cells by the Use of Secondary Ammonium Cations, *ACS Energy Lett.* **2020**, 5, 1013−1021.

[2] Nishimura, K.; Kamarudin, M. A.; Hirotani, D.; Hamada, K.; Shen, Q.; Iikubo, S.; Minemoto, T.; Yoshino, K.; Hayase, S., Lead-free tin-halide perovskite solar cells with 13% efficiency. *Nano Energy* **2020,** 74, 104858.

[3] Jiang, X.; Wang, F.; Wei, Q.; Li, H.; Shang, Y.; Zhou, W.; Wang, C.; Cheng, P.; Chen, Q.; Chen, L.; Ning, Z., Ultra-high open-circuit voltage of tin perovskite solar cells via an electron transporting layer design. *Nature Communications* **2020,** 11, 1245.